

High resolution carbon isotope stratigraphy across the Cenomanian/Turonian boundary in the Tappu area, Hokkaido, Japan: correlation with world reference sections

¹Takashi HASEGAWA, ²Sohhei SEO, ³Kazuyoshi MORIYA,
⁴Yoshito TOMINAGA, ⁴Toshifumi NEMOTO and ⁴Takahiro NARUSE

1. *School of Natural System, Institute of Science and Engineering, Kanazawa University, Kakuma-machi, Kanazawa 920-1192 Japan*
Email: jh7ujr@kenroku.kanazawa-u.ac.jp
Phone: +81-76-264-6508, Fax: +81-76-264-6545
2. *Faculty of Science, Kanazawa University, Kakuma-machi, Kanazawa 920-1192 Japan*
3. *Department of Earth Sciences, Faculty of Education and Integrated Arts and Sciences, Waseda University, Tokyo 169-8050 Japan*
4. *Graduate School of Natural Science and Technology, Kanazawa University Kakuma-machi, Kanazawa 920-1192 Japan*

(Received March 2, 2010 and accepted in revised form March 11, 2010)

Abstract High resolution carbon isotope stratigraphy encompassing the Cenomanian/Turonian boundary in the Tappu section, Hokkaido, Japan enables correlations to be made with Eastbourne and Pueblo world reference sections. The organic carbon in the sedimentary rocks of the Yezo Group is derived predominantly from terrestrial higher plants. The stratigraphic profiles of carbon isotope values in the Tappu section show remarkable variations. A brief and small peak in the lower part, an extended plateau-shaped peak with larger magnitude in the upper part, and a trough dividing the two peaks observed in the Tappu section are well known patterns for the isotope profiles of the reference sections. Close similarity of the patterns among these regions validates a precise correlation of the Japanese Cenomanian/Turonian boundary sequence with the international standard reference sections in North Atlantic and Western Interior Sea regions.

Key words: Cenomanian, Turonian, OAE, Carbon isotopes, Cretaceous, Organic carbon

Introduction

Cretaceous oceanic anoxic events (OAEs) are well known oceanic events typically represented by organic-rich dark sediments (e.g. Arthur and Premoli Silva 1982, Arthur et al. 1987, Schlanger et al. 1987). During OAEs, large quantities of organic carbon have been deposited and have not been recycled because of expanded anoxic bottom water masses (Schlanger and Jenkyns 1976, Arthur and Schlanger 1979). We can interpret an OAE as a short-term departure from the steady state of carbon cycling that fluctuates with a wavelength of several million years (Kump and Arthur 1999). The OAE recorded across the Cretaceous Cenomanian/Turonian (C/T) boundary is called Oceanic Anoxic Event 2 (OAE2; Arthur and Schlanger 1979) and is known for its wide-reaching oceanic anoxia that affected most of the world (Arthur et al. 1987, Schlanger et al. 1987). The intensity of OAE2 is believed to have been the strongest among the Cretaceous OAEs in terms of its oxygen deficiency and global extent (e.g. Schlanger et al. 1987, Arthur and Schlanger 1979). A positive 2-3 ‰ excursion of carbon isotope ratios ($\delta^{13}\text{C}$) derived from the perturbation of carbon cycling characterizes the OAE2 well, and it often is employed as an interregional chemostratigraphic marker (e.g. Hasegawa 1997, Paul et al. 1999, Pratt 1985, Voigt et al. 2007). Carbonate carbon has been employed for isotope studies for pelagic carbonate sequences in Tethys, the North Atlantic and the Western Interior Sea of North America; whereas, terrestrial organic carbon is the target material for clastic sequences of the Western Pacific (e.g. Hasegawa 1997, Hasegawa et al. 2003).

Recent progress in C-isotope stratigraphy in European sections shows a detailed pattern of OAE2 fluctuation through the uppermost Cenomanian (Paul et al. 1999, Voigt et al. 2007). Previous studies of C-isotope stratigraphy on the Yezo Group along the Kanajiri River (Tappu section) showed a conspicuous positive excursion across the C/T boundary (Hasegawa and Saito 1993, Uramoto et al. 2009). At the Hasegawa Laboratory of Kanazawa University, we have studied C-isotope stratigraphy across the C/T boundary through the Tappu section and published preliminary results (Moriya et al. 2008). We could correlate the section with the reference section at Dover, UK, and with the high mass accumulation rates (~ 400 m/myr) of the Tappu section, we were able to achieve higher stratigraphic resolution. From a global perspective, high resolution C-isotope stratigraphy, along with detailed correlations with the world reference sections, is fundamental for investigations on OAE2 from the Yezo Group.

The objective of this study is to establish the C-isotope stratigraphy through the range equivalent to the OAE2 interval with the world's highest resolution from Japanese land sections, and to describe the isotope profiles. Basic lithology near the C/T boundary also is described.

Materials and methods

Stratigraphically dense samples with stratigraphic intervals of 2-5 m along the

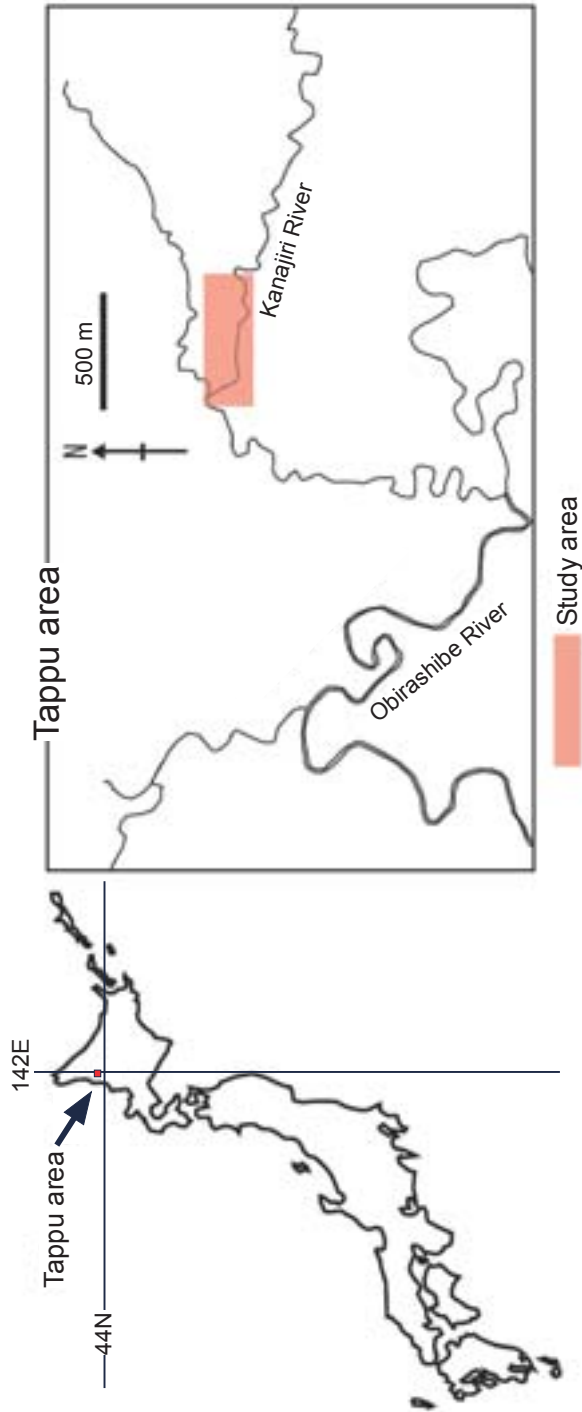


Fig. 1 Index map showing the study area along the Kanajiri River, a tributary of the Obirashibe River in the Tappu area, Obira Town, Hokkaido, Japan.

Kanajiri River in the Tappu area, Hokkaido, Japan (Fig. 1) were collected from the lower part of the Saku Formation (Takashima et al. 2004) (Fig. 2). The lower part of the section is characterized by mudstone to sandy mudstone. Common intercalations of fine to very fine sandstone layers of distal turbidites are observed through 120 m from the base of the column. The upper part of the section is mainly composed of bioturbated sandy mudstone with occasional intercalation of thin, very fine sandstone to sandy mudstone layers. An interval of about 3.5 m of coarsening with indurated, stratified, very fine sandstone to sandy siltstone was observed around 270 m in the upper part. The C/T boundary marker bed described below is located about 0.5 m below this interval. Tuff layers thicker than 20 cm are common in the upper part of the section. See Moriya et al. (2008) for details of the lithology of the study area.

Organic compositions of 16 selected mudstone samples (indicated with * on Table 1 and with light-blue circular highlights in Fig. 2) were checked by visual observation of kerogen under reflected light and in fluorescent light. Crushed mudstone material was made into polished blocks following standard preparation procedures (Bustin et al. 1983). Polished pellets were examined under the microscope to identify organic particles.

Powdered mudstones were obtained from fresh rock surfaces using a dental grinder and were treated with 5M HCl for 12 hours to remove carbonate minerals. After repeated rinsing with deionized water to remove Cl⁻, each neutralized sample was dried and approximately 2-4 mg of the sample was placed in a tin film cup and weighed. The samples were then introduced into a Thermo Finnigan elemental analyzer (EA) Flash 1112 at the Center for Advanced Marine Core Research of Kochi University. Each sample was combusted at 900 °C and the sample-derived CO₂ was then transferred into an EA-connected Delta Plus Advantage mass spectrometer for δ¹³C analyses. The results reported herein were obtained using reference CO₂ calibrated by ANU-sucrose directly and NBS-19 indirectly. Each data point is an average of multiple (more than three) analyses for each sample, and is expressed in the conventional delta notation with respect to the VPDB standard, where $\delta^{13}\text{C}(\text{‰}) = [({}^{13}\text{C}/{}^{12}\text{C})_{\text{sample}} / ({}^{13}\text{C}/{}^{12}\text{C})_{\text{standard}} - 1] \times 1000$. The isotopic values were checked by isotopically well-characterized laboratory standards. Repeated analysis of a laboratory standard indicates ±0.2‰ as the instrumental reproducibility for a single analysis.

Results

The composition of kerogens in all selected samples shows the predominance of semifusinite or vitrinite, from terrestrial origins. Associated with these kerogens, minor (<1 %) content of cutinite and liptinite, including sporinite and possible alginite with weak yellow fluorescence, was observed in some samples.

All δ¹³C values obtained in this study are summarized in Table 1. The δ¹³C values are consistent around -24.7‰ at the lower part of the section, between 43.6 m (KZZ-016)

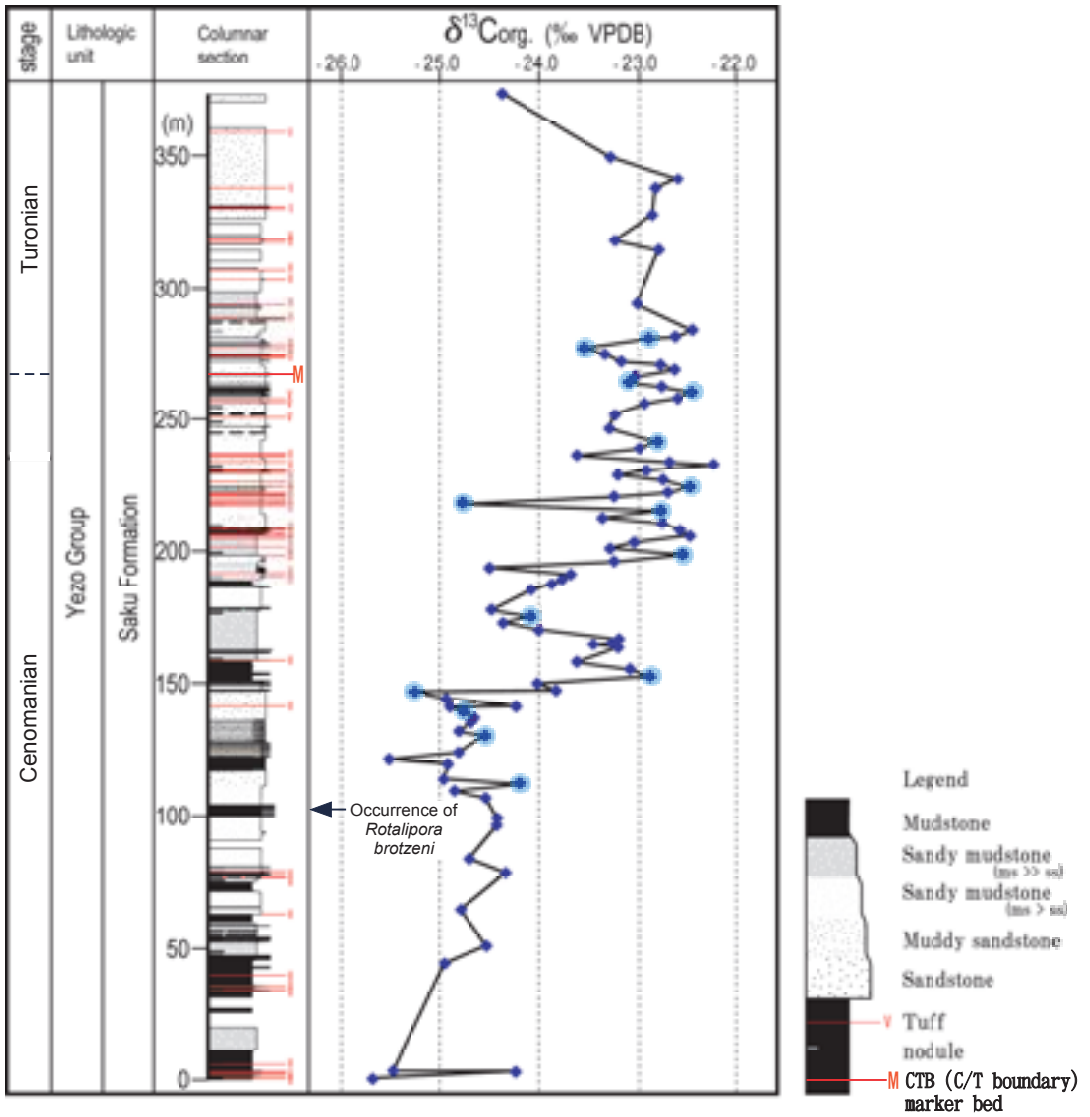


Fig. 2 Geologic column and carbon isotope stratigraphy through the studied section. Data points highlighted by light-blue circles indicate samples on which microscopic observations were performed to corroborate the terrestrial origin of organic matter. Note rapid positive shift around 150 m and negative shift-back around 175 m. Occurrence of planktonic foraminifera (*Rotalipora brotzeni*) is indicated with an arrow. The species does not indicate latest Cenomanian dates. Details of the foraminiferal study will be published elsewhere.

Sample	Thickness separation from KZZ- 001 (m)	$\delta^{13}\text{C}_{\text{org.}}$ (‰ VPDB)	Sample	Thickness separation from KZZ- 001 (m)	$\delta^{13}\text{C}_{\text{org.}}$ (‰ VPDB)	Sample	Thickness separation from KZZ- 001 (m)	$\delta^{13}\text{C}_{\text{org.}}$ (‰ VPDB)
KZZ064	154.9	-23.09	KZZ096	230.0	-22.92	KZZ-142	372.6	-24.38
KZZ063*	152.2	-22.89	KZZ095	228.2	-23.21	KZZ-140	348.6	-23.29
KZZ062	149.5	-24.02	KZZ094	226.5	-22.76	KZZ-139	340.3	-22.61
KZZ061	146.9	-23.83	KZZ093*	223.7	-22.48	KZZ-138	336.7	-22.83
KZZ060*	146.1	-25.26	KZZ092	221.7	-22.71	KZZ-135	326.7	-22.86
KZZ059	143.7	-24.94	KZZ091	220.2	-23.25	KZZ-132	317.0	-23.24
KZZ058	140.9	-24.25	KZZ090*	217.6	-24.77	KZZ-131	313.5	-22.80
KZZ057	140.8	-24.90	KZZ089*	214.6	-22.78	KZZ-125	293.1	-23.02
KZZ056*	138.9	-24.76	KZZ088	212.0	-23.37	KZZ-121	283.2	-22.47
KZZ055	136.6	-24.66	KZZ087	209.9	-22.76	KZZ-120	280.7	-22.63
KZZ054	134.9	-24.69	KZZ086	207.3	-22.59	KZZ119*	279.8	-22.90
KZZ052	131.5	-24.81	KZZ085	205.1	-22.49	KZZ117*	276.3	-23.55
KZZ051*	129.6	-24.55	KZZ084	202.8	-23.05	KZZ116	274.0	-23.34
KZZ049	123.4	-24.82	KZZ083	200.4	-23.29	KZZ115	271.2	-23.18
KZZ048	120.9	-25.52	KZZ082*	198.0	-22.56	KZZ114	269.9	-22.78
KZZ047	119.0	-24.93	KZZ081	195.7	-23.25	KZZ113	268.1	-22.64
KZZ045	113.3	-24.97	KZZ080	193.2	-24.51	KZZ112	265.6	-23.04
KZZ044*	111.6	-24.20	KZZ079	190.8	-23.68	KZZ111*	263.4	-23.10
KZZ043	108.9	-24.86	KZZ078	188.8	-23.77	KZZ110	261.8	-22.77
KZZ042	106.2	-24.55	KZZ077	187.1	-23.88	KZZ109*	259.6	-22.47
KZZ039	98.5	-24.43	KZZ076	184.9	-24.09	KZZ108	257.4	-22.61
KZZ038	95.7	-24.44	KZZ073	177.3	-24.49	KZZ107	255.5	-22.94
KZZ033	83.2	-24.71	KZZ072*	174.6	-24.09	KZZ105	251.1	-23.24
KZZ031	77.9	-24.35	KZZ071	172.3	-24.37	KZZ103	246.0	-23.30
KZZ025	63.9	-24.79	KZZ070	169.6	-24.01	KZZ101*	240.8	-22.81
KZZ019	50.3	-24.54	KZZ069	166.2	-23.20	KZZ100	238.4	-23.00
KZZ016	43.6	-24.96	KZZ068	164.7	-23.28	KZZ099	235.8	-23.62
KZZ004	3.0	-25.48	KZZ067	164.2	-23.46	KZZ098	233.1	-22.69
KZZ003	2.7	-24.25	KZZ066	162.9	-23.21	KZZ097	232.2	-22.24
KZZ001	0.0	-25.68	KZZ065*	157.6	-23.62			

Each sample horizon is indicated in thickness separation from KZZ-001.

Sample names with astalisks indicate samples that are micriscopically observed for organic composition.

Table 1 Carbon isotope values of studied samples in the Tappu section, Hokkaido, Japan.

and 146.1 m (KZZ-060). Then the values shift in the positive direction and reach -22.89‰ at 152m (KZZ-063). The values gradually shift back in the negative direction and reach the lowest point at 177.3 m (KZZ-073). The trend reverses here, where the $\delta^{13}\text{C}$ values start a gradual positive shift toward 198.0 m (KZZ-082). Once $\delta^{13}\text{C}$ values reach around -22.9‰, they remain similar through the extended range. Thus the trend is that of a plateau through the upper half of the studied section. However, at the top of the section, the $\delta^{13}\text{C}$ values drop significantly and reach -24.38‰. Some horizons (i.e. at 2.7 m, 193.2 m and 217.6 m; KZZ-003, -080 and -090 respectively) have irregular positive or negative spikes, larger than 1‰, which are not concordant with the general trend of the $\delta^{13}\text{C}$ curve.

The profile of carbon isotope values obtained in this study (Fig. 2) shows the characteristic double-peaked positive excursion of 2.5-3‰ with a dividing trough. A relatively sharp peak near 150 m comprises the first peak, and a plateau-like stable range constitutes a second peak. The trough drops to two-thirds to three-fourths of the value of the first peak. The second peak is four or five times more expanded in stratigraphic thickness than the first peak or the trough. The maximum $\delta^{13}\text{C}$ value in this section was recorded within the second peak interval.

Discussion

The organic matter in each sample was derived predominantly from terrestrial woody plants. All previous studies, which have analyzed organic components in mudstones of the Yezo Group, including some along the Kanajiri River (Hasegawa 2001, Hasegawa and Saito 1993, Uramoto *et al.* 2009), show a predominance of material from terrestrial origins, and a high marine organic content has never been reported. Therefore, the isotope stratigraphy in this study reflects fluctuations of $\delta^{13}\text{C}$ of higher plants, which photosynthesized from atmospheric CO_2 during the depositional period. Because atmospheric CO_2 is interpreted to have been C-isotopically equilibrated with dissolved CO_2 in sea surface water, the carbonate carbon precipitated from CO_3^{2-} , which also was C-isotopically equilibrated with the dissolved CO_2 , should show the same fluctuations (Hasegawa 1997, Hasegawa 2003).

Regardless of some irregular spikes, the general trend of the $\delta^{13}\text{C}$ curve clearly exhibits a positive excursion composed of double peaks. The first peak reflects an apparent prompt onset, but the duration is brief and the peak value is not as positive as that of the second peak. The peaks are comparable to a diagnostic feature for $\delta^{13}\text{C}$ patterns of the OAE2 horizon (Paul *et al.* 1999, Pratt 1985, Snow *et al.* 2005), and indicate that our $\delta^{13}\text{C}$ profile can be correlated to the world reference sections (Fig. 3). Paul *et al.* (1999) subdivided the isotope profile across the C/T boundary into six segments, which included the Pre excursion (PrE), First build-up (1BU), Trough interval (TI), Second build-up (2BU), Plateau (PL) and Recovery (RC). All of these phases can be recognized in the Tappu section, as mentioned by Moriya *et al.* (2008). In this study, we

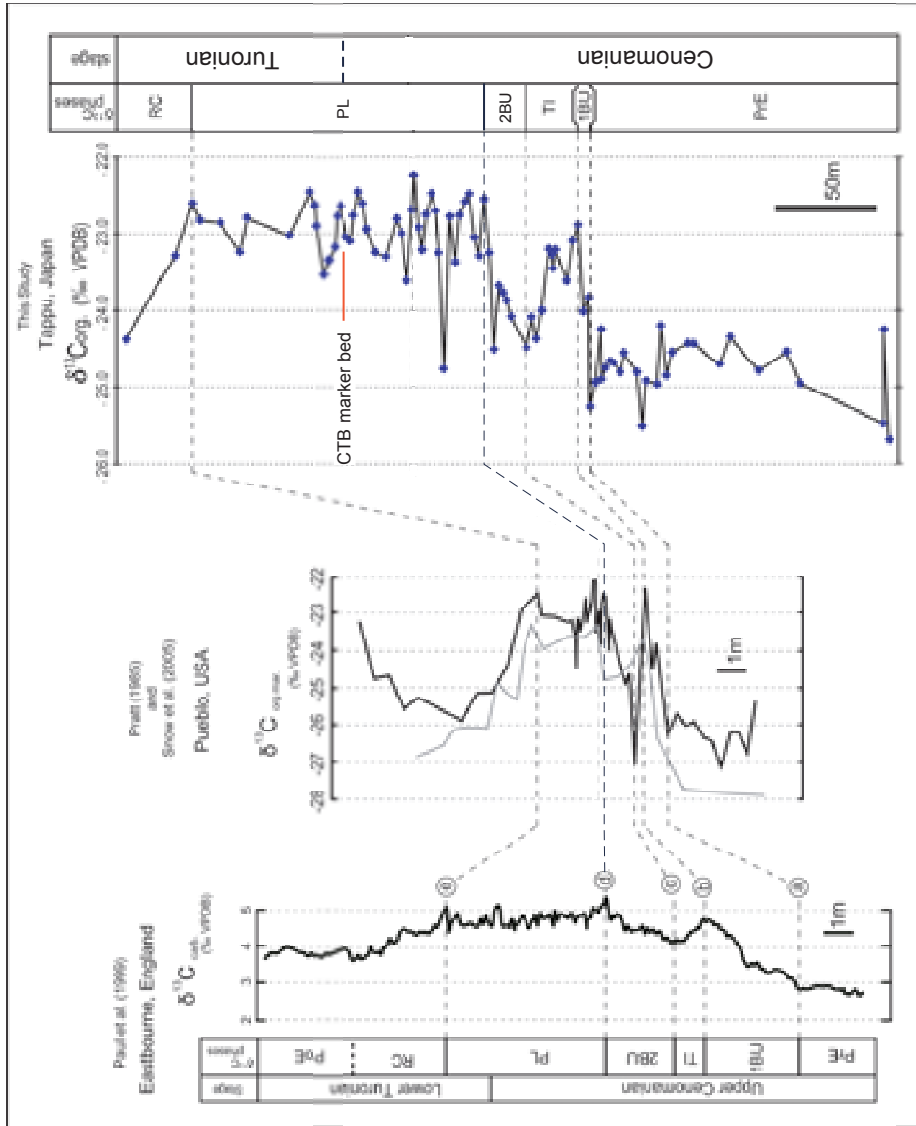


Fig. 3 Comparisons of carbon isotope profiles from world reference sections, specifically Eastbourne, UK (Paul et al. 1999) and Pueblo, USA (Pratt 1985, Snow et al. 2005) and the Tappu section (this study). Note that all $\delta^{13}C$ phases (Paul et al. 1999) are recognized through the Tappu section. The phase boundaries are alphabetically marked and tied between the sections.

could designate the correlated horizon of each phase boundary more precisely with a higher resolution data set (lines a-e in Fig. 3). Sageman *et al.* (2006) established an orbital time scale across the C/T boundary at the Pueblo section. They estimated that the duration of the carbon isotope excursion (from 1BU to near the top of PL) was 538 kyr. Correlation between the Tappu and Pueblo sections enables us to extrapolate this duration onto the Tappu section. It is inferred that the mean time resolution of our samples is greater than 10 kyr.

Hasegawa and Saito (1993) studied C-isotope stratigraphy across the C/T boundary along the Kanajiri River, and recognized double peak excursions of which the “first peak” was composed of a single data point. Recently, Uramoto *et al.* (2009) studied the same section, but did not collect samples from the stratigraphic range of the “first peak” (recognized by Hasegawa and Saito, 1993). Uramoto *et al.* (2009) plotted their original data with data of Hasegawa and Saito (1993) to construct a C-isotope profile. Consequently, the “first peak” is found in their profile and three peaks are recognized within it. Conversely, we collected a planktonic foraminiferal species (*Rotalipora brotzeni*) above this “first peak” horizon. There are two reasons why the “first peak” observed by Hasegawa and Saito (1993) is not correlated to the real first peak in the reference section. These reasons are: (1) The Last Appearance Datum of this species is located in the middle of the *Rotalipora cushmani* Zone (Caron 1985). (2) The first peak recognized at the Eastbourne section is observed at the uppermost part of *R. cushmani* Zone. Furthermore, our $\delta^{13}\text{C}$ data across the “first peak” horizon (corresponding to ~95 m in this study) did not show any positive excursions. Therefore, we conclude that the single data point that made the “first peak” in Hasegawa and Saito (1993) was erroneous. The real first peak in the Tappu section is represented by samples KZZ-063-069 (152.2-166.2 m) in this study, and appears to correspond to the second peak of Uramoto *et al.* (2009).

We tried to estimate the horizon of the C/T boundary in the studied section from the C-isotope stratigraphy as it could not be identified by biostratigraphy alone (Uramoto *et al.* 2009). The biostratigraphically defined C/T boundary at the Pueblo section appears to be located at the top of the PL (Sageman *et al.* 2006) or within the PL (Keller *et al.* 2004, Snow *et al.* 2005); whereas, it is located just above a ~0.4‰ positive excursion within the PL in the Eastbourne section (Jarvis *et al.* 2006). In the Tappu section, we could not identify the positive 0.4‰ excursion since there are four positive excursions within the PL. Consequently, the C/T boundary could not be extrapolated based on C-isotope stratigraphy, even though the “range” in which the real C/T boundary was located has been narrowed. Nevertheless, we draw the provisional C/T boundary just above “CTB (C/T boundary) marker bed”. The bed is stratigraphically located in the middle of the PL and it is interpreted to be very close to the real C/T boundary (Fig. 3). The marker bed is convenient for further studies across the C/T boundary along the Kanajiri River section since the beds are very conspicuous, unique, and easy to recognize (Figs. 4, 5).

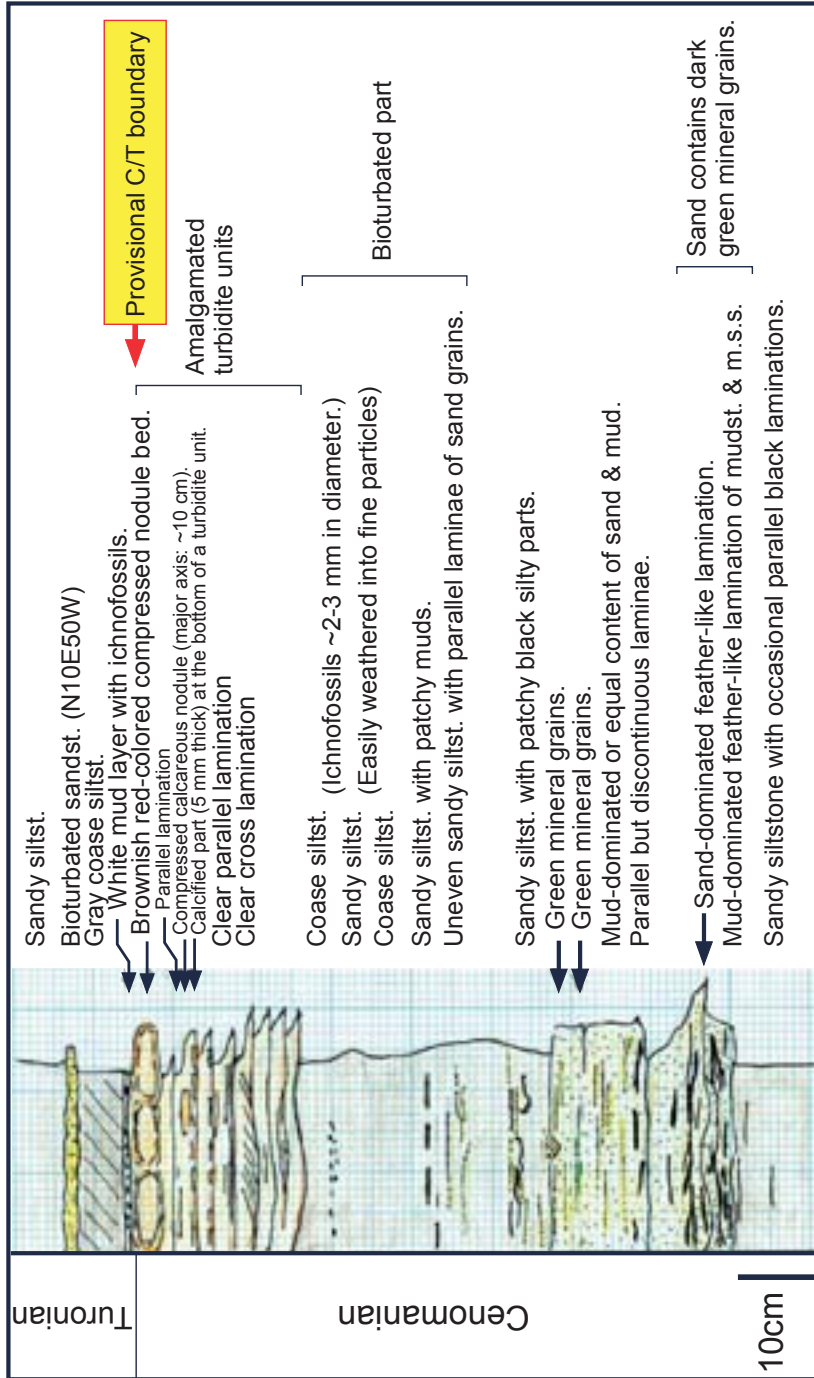


Fig. 4 Lithology of “CTB (C/T boundary) marker bed”. A remarkable, characteristic sedimentary sequence is observed in the middle of PL (“Plateau” phase of C- isotope profile). Stratigraphic position of the marker bed is interpreted to be close to the real C/T boundary. A provisional C/T boundary along the Kanajiri River is drawn just above a conspicuous, compressed nodular bed.

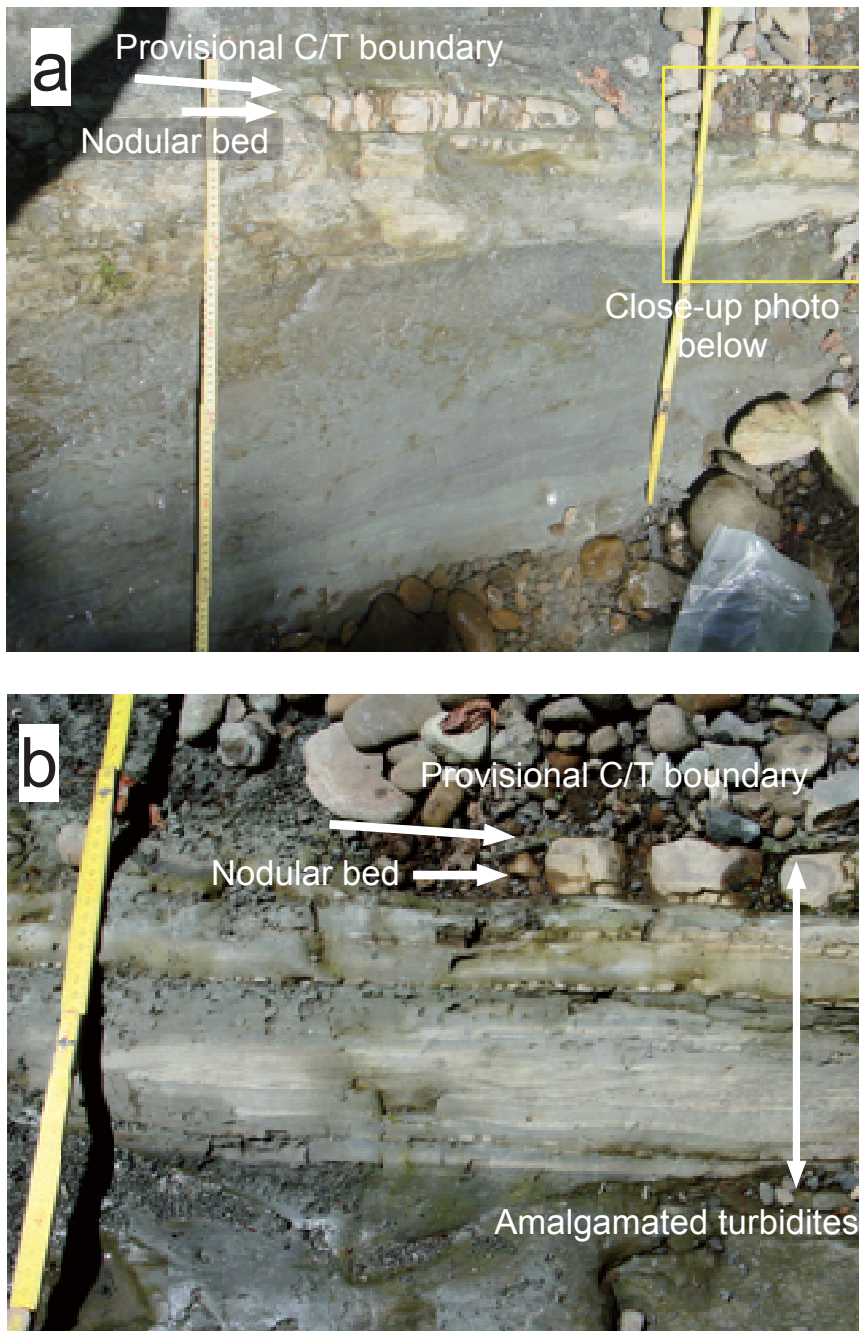


Fig. 5 Outcrop of “CTB marker bed” described in Fig. 4. a) Entire sequence of “CTB marker bed” and b) Close-up photo of amalgamated turbidites.

Some negative and positive events observed in the middle of the PL are composed of multiple data points and appear to be meaningful events rather than errors or noises (Fig. 2). We suggest that smaller $\delta^{13}\text{C}$ events observed in the Eastbourne and Pueblo sections could be correlatable to the Tappu section. Higher resolution studies in both of the world reference sections and the Tappu section could increase tie points between the sections to establish an orbital scale of global correlations.

Summary

Carbon isotope stratigraphy across the C/T boundary in the Yezo Group was studied with higher resolution than any previous studies. As a result, the data set obtained in this study enables us to correlate OAE2-corresponding intervals of the Pacific Tappu section with those of well-studied European sections with five tie lines (Fig 3. a-e). Such precise correlation, along with a description of the CTB marker bed, provides fundamental information that is beneficial for further comparative OAE2 studies from a global view point. LIP formation was discussed as a causal event of OAE2 from other sections of the world, based on Pb and Os isotopes and other geochemical data with stratigraphic control of detailed carbon isotope stratigraphy (Kuroda et al. 2007, Snow et al. 2005, Turgeon and Creaser 2008). On the other hand, Voigt et al. (2006) considered the extensive cooling derived from perturbation of carbon circulation during OAE2. The Pacific Tappu section is an excellent section for international correlation and potentially provides much higher stratigraphic resolution than counterpart world reference sections. Thus, this section may provide a valuable reference for studying events associated with OAE2, and may help identify their causal relationships within the OAE2 interval.

Acknowledgments

The authors express their deep appreciation to Prof. T. Kamiya of the Kanazawa University for their constructive suggestions during the review process, and Dr. Y. Suzuki of the Geological Survey of Japan for his kind assistance and helpful suggestions during microscopic observations at his laboratory. This study was performed under the cooperative research program of the Center for Advanced Marine Core Research (CMCR), Kochi University (Accept No.06B021, 07A008, 07B007). This study was financially supported by Grants-in-Aid for Scientific Research nos. 18340164, 20403016, 20340144 from JSPS (to T. Hasegawa).

References

- Arthur, M. A. and Premoli Silva, I. (1982) Development of widespread organic carbon-rich strata in the Mediterranean Tethys. In *Nature and origin of Cretaceous carbon-rich facies*, Eds. M. A. Arthur & M. B. Cita Academic Press, pp 7-54. New York.

- Arthur, M. A. and Schlanger, S. O. (1979) Cretaceous "Oceanic Anoxic Events" as causal factors in development of reef-reservoired giant oil fields. *American Association of Petroleum Geologists Bulletin*, **63**, 870-885.
- Arthur, M. A., Schlanger, S. O. and Jenkyns, H. C. (1987) The Cenomanian-Turonian Oceanic Anoxic Event, II. Palaeoceanographic controls on organic-matter production and preservation. In *Marine Petroleum Source Rocks*, Eds. J. Brooks & A. J. Fleet Geological Society Special Publication 26, pp 401-420.
- Bustin, R. M., Cameron, A. R., Grieve, D. A. and Kalkreuth, W. D. (1983) Coal petrology, its principles, methods, and applications. In *Geological Association of Canada, Short Course Note 3*, Geological Association of Canada, pp 230-233. Victoria.
- Caron, M. (1985) Cretaceous planktic foraminifera. In *Plankton Stratigraphy*, Eds. H. M. Bolli, J. B. Saunders & K. Perch-Nielsen Cambridge University Press, pp 17-86. Cambridge.
- Hasegawa, T. (1997) Cenomanian-Turonian carbon isotope events recorded in terrestrial organic matter from northern Japan. *Palaeogeography, Palaeoclimatology, Palaeoecology*, **130**, 251-273.
- Hasegawa, T. (2001) Predominance of terrigenous organic matter in Cretaceous marine fore-arc sediments, Japan and Far East Russia. *International Journal of Coal Geology*, **47**, 207-221.
- Hasegawa, T. (2003) Cretaceous terrestrial paleoenvironments of northeastern Asia suggested from carbon isotope stratigraphy: Increased atmospheric pCO₂-induced climate. *Journal of Asian Earth Sciences*, **21**, 849-859.
- Hasegawa, T., Pratt, L. M., Maeda, H., Shigeta, Y., Okamoto, T., Kase, T. and Uemura, K. (2003) Upper Cretaceous stable carbon isotope stratigraphy of terrestrial organic matter from Sakhalin, Russian Far East: a proxy for the isotopic composition of paleoatmospheric CO₂. *Palaeogeography, Palaeoclimatology, Palaeoecology*, **189**, 97-115.
- Hasegawa, T. and Saito, T. (1993) Global synchronicity of a positive carbon isotope excursion at the Cenomanian/Turonian boundary: validation by calcareous microfossil biostratigraphy of the Yezo Group, Hokkaido, Japan. *Island Arc*, **2**, 181-191.
- Jarvis, I., Gale, A. S., Jenkyns, H. C. and Pearce, M. A. (2006) Secular variation in Late Cretaceous carbon isotopes: A new $\delta^{13}\text{C}$ carbonate reference curve for the Cenomanian-Campanian (99.6-70.6 Ma). *Geological Magazine*, **143**, 561-608.
- Keller, G., Berner, Z., Adatte, T. and Stueben, D. (2004) Cenomanian-Turonian and $\delta^{13}\text{C}$, and $\delta^{18}\text{O}$, sea level and salinity variations at Pueblo, Colorado. *Palaeogeography, Palaeoclimatology, Palaeoecology*, **211**, 19-43.
- Kump, L. R. and Arthur, M. A. (1999) Interpreting carbon-isotope excursions: carbonate and organic matter. *Chemical Geology*, **161**, 181-198.
- Kuroda, J., Ogawa, N. O., Tanimizu, M., Coffin, M. F., Tokuyama, H., Kitazato, H. and Ohkouchi, N. (2007) Contemporaneous massive subaerial volcanism and late Cretaceous

- Oceanic Anoxic Event 2. *Earth and Planetary Science Letters*, **256**, 211–223.
- Moriya, K., Hasegawa, T., Naruse, T., Seo, S., Nemoto, T., Suzuki, T. and Morimoto, K. (2008) Ultra-high resolution analyses of foraminiferal fossil assemblages for the Cenomanian/Turonian boundary (mid-Cretaceous) extinction interval. *Chigaku-zasshi*, **117**, 878-888 (in Japanese with English abstract).
- Paul, C. R. C., Lamolda, M. A., Mitchell, S. F., Vaziri, M. R., Gorostidi, A. and Marshall, J. D. (1999) The Cenomanian-Turonian boundary at Eastbourne (Sussex, UK): a proposed European reference section. *Palaeogeography, Palaeoclimatology, Palaeoecology*, **150**, 83-121.
- Pratt, L. M. (1985) Isotopic studies of organic matter and carbonate in rocks of the Greenhorn marine cycle (USA). In *Fine-grained deposits and biofacies of the Cretaceous Western Interior Seaway. Field trip, Golden, CO, 1985*, Eds. L. M. Pratt, E. G. Kauffman & B. Z. Frederick Society of Economic Petrologists and Mineralogists, pp 38-48. Tulsa.
- Sageman, B. B., Meyers, S. R. and Arthur, M. A. (2006) Orbital time scale and new C-isotope record for Cenomanian-Turonian boundary stratotype. *Geology*, **34**, 125-128.
- Schlanger, S. O., Arthur, M. A., Jenkyns, H. C. and Scholle, P. A. (1987) The Cenomanian-Turonian Oceanic Anoxic Event, I. Stratigraphy and distribution of organic carbon-rich beds and the Marine delta 13C excursion. In *Marine Petroleum Source Rocks*, Geological Society Special Publication 26, pp 371-399. London.
- Schlanger, S. O. and Jenkyns, H. C. (1976) Cretaceous oceanic anoxic events: causes and consequences. *Geologie en Mijnbouw*, **55**, 179-184.
- Snow, L. J., Duncan, R. A. and Bralower, T. J. (2005) Trace element abundances in the Rock Canyon Anticline, Pueblo, Colorado, marine sedimentary section and their relationship to Caribbean plateau construction and ocean anoxic event 2. *Paleoceanography*, **20**, 1-14.
- Takashima, R., Kawabe, F., Nishi, H., Moriya, K., Wani, R. and Ando, H. (2004) Geology and stratigraphy of forearc basin sediments in Hokkaido, Japan: Cretaceous environmental events on the north-west Pacific margin. *Cretaceous Research*, **25**, 365-390.
- Turgeon, S. C. and Creaser, R. A. (2008) Cretaceous oceanic anoxic event 2 triggered by a massive magmatic episode. *Nature*, **454**, 323-326. doi:10.1038/nature07076.
- Uramoto, G. I., Abe, Y. and Hirano, H. (2009) Carbon isotope fluctuations of terrestrial organic matter for the Upper Cretaceous (Cenomanian - Santonian) in the Obira area of Hokkaido, Japan. *Geological Magazine*, **146**, 761-774.
- Voigt, S., Aurag, A., Leis, F. and Kaplan, U. (2007) Late Cenomanian to Middle Turonian high-resolution carbon isotope stratigraphy: New data from the Münsterland Cretaceous Basin, Germany. *Earth and Planetary Science Letters*, **253**, 196-210.
- Voigt, S., Gale, A. S. and Voigt, T. (2006) Sea-level change, carbon cycling and palaeoclimate during the Late Cenomanian of northwest Europe; an integrated palaeoenvironmental analysis. *Cretaceous Research*, **27**, 836-858.